# Numerical Study of the Apodization Profile Functions, Optimal Profiles and Lengths of a Linearly Chirped Fibre Bragg Grating *

QIN Zi-Xiong (秦子雄)[1,2], ZENG Qing-Ke (曾庆科)[1,2], FENG De-Jun (冯德军)[1], XIANG Yang(项阳)[1], DING Lei (丁镭)[1], KAI Gui-Yun (开桂云)[1], LIU Zhi-Guo (刘志国)[1], YUAN Shu-Zhong (袁树忠)[1], DONG Xiao-Yi (董孝义)[1], LIU Ning (刘宁)[3], LIAO Chang-Jun (廖常俊)[3], LIU Song-Hao (刘颂豪)[3]

[1]*Institute of Modern Optics, Nankai University, Tianjin 300071*

[2]*Department of Physics, Guangxi Normal University, Guilin 541004*

[3]*Institute of Quantum Electronics, South China Normal University, Guangzhou 510631*

(Received 21 June 2000)

*Starting from our definition of apodization profile functions, we discover the optimal profiles and the characteristics of defined apodization functions in sidelobe suppression. It is shown by numerical analysis that the optimal grating length is 45 mm to compensate for dispersion induced by 100 km fibres and the smoothness of the ripples in time-delay characteristics is related to the defined parameters.*

*PACS: 42. 79. Dj, 42. 79. Sz, 42. 81. Qb*

Since the discovery of photosensitivity in single mode optical fibres and the production of in-core Bragg grating reflectors,[1] many techniques have been refined and developed to permit the production of efficient fibre Bragg gratings with well-controlled parameters. Numerous applications have been proposed for these elements. As dispersion cancelling elements, they are very attractive as they are linear passive devices, highly dispersive, compact and relatively easy to fabricate in large numbers.

The ideal dispersion compensator of optical fibres is required to have a linear time delay characteristic. That is, the relative delays for the various frequency components contained in the optical pulse should be linear across the bandwidth of the pulse. Unfortunately, the Bragg grating with a linear chirp may have an oscillatory time-delay characteristic. It is shown that the oscillations in the time-delay characteristic can be reduced (smoothed) to provide a more linear time-delay response by apodizing the Bragg reflector.[2] Meanwhile, apodization also has the effect of reducing the sidelobes in the spectral reflection response of a Bragg grating. Apodization consists of photoinducing a refractive index modulation with an amplitude along the length of the gratings that has a bell-like function shape and with an average pitch equal to the desired Bragg centre-resonance wavelength $\lambda_0$ divided by twice the effective mode index. Apodization has received considerable attention.[3] In general, the bell-like function is considered as the Gaussian functions or window functions in traditional filter theory, but it is not sufficient in some circumstances. In this letter, starting from our defined apodization profile functions, we will analyse the profile functions and numerically study the relation among the length of the grating, the chirp amount, sidelobe suppression and the profile functions.

Fibre Bragg gratings are produced by exposing an optical fibre to a spatially varying pattern of ultraviolet intensity. For simplicity, here we assume that what results is a perturbation to the effective refractive index of the guided mode of interest,[4] described by $\delta n_{\rm eff}(Z) = \overline{\delta} n_{\rm eff}(Z)\{1 + V\cos[2\pi Z/\Lambda + \Psi(Z)]\}$, where $\overline{\delta} n_{\rm eff}(Z)$ is the dc index change spatially averaged over a grating period, $V$ is the fringe visibility of the index, $\Lambda$ is the nominal period, and $\Psi(Z)$ describes the grating chirp.

For modelling apodized gratings, starting from the coupled-mode theory, we calculate the reflectivity and time delay using the transfer matrix technique.[5] The grating is divided into a number of segments, each having a constant period, phase and apodization corresponding to their values at the segment mid-point. $\overline{\delta} n_{\rm eff}(Z)$ can be assumed to take any shape of functions to have different apodization profiles. We define the following apodization profile functions:

$$\overline{\delta} n_{\rm eff}(Z) = \begin{cases} \overline{\delta} n_{\rm eff}\left\{1 + \dfrac{T_1}{4} - T_1\left[\dfrac{[Z-(1-F)L/2]}{LF}\right]^2\right\} & \\ \cdot(1+\dfrac{T_1}{4})^{-1}, & Z > L(1-F)/2, \\ \overline{\delta} n_{\rm eff}, & |Z| \le L(1-F)/2, \\ \overline{\delta} n_{\rm eff}\left\{1 + \dfrac{T_1}{4} - T_1\left[\dfrac{Z+(1-F)L/2}{LF}\right]^2\right\} & \\ \cdot(1+\dfrac{T_1}{4})^{-1}, & Z < -L(1-F)/2, \end{cases} \tag{1}$$

$$\overline{\delta} n_{\rm eff}(Z) = \overline{\delta} n_{\rm eff} \exp\left[-\left(\frac{4Z^2\ln 2}{T_0^2}\right)^m\right], \tag{2}$$

*Supported by 863 National High Technology Research Plan (863-307-15), Tianjin Natural Science Foundation(003600811), China Postdoctoral Science Foundation and Huawei Scientific Research Foundation.

©2001 Chinese Physical Society and IOP Publishing Ltd

$$\overline{\delta}n_{\rm eff}(Z)=\begin{cases}-\overline{\delta}n_{\rm eff}\tanh[T_1(Z-\dfrac{L}{2})], & Z\geq 0,\\ \overline{\delta}n_{eff}\tanh[T_1(Z+\dfrac{L}{2})], & Z<0,\end{cases} \tag{3}$$

$$\overline{\delta}n_{\rm eff}(Z)=\begin{cases}\overline{\delta}n_{\rm eff}\{0.5+0.5\cos[\dfrac{2\pi}{LF}(Z\\ -\dfrac{L}{2}(1-F))]\}, & Z>L(1-F)/2,\\ \overline{\delta}n_{\rm eff}, & |Z|\leq L(1-F)/2,\\ \overline{\delta}n_{\rm eff}\{0.5+0.5\cos[\dfrac{2\pi}{LF}(Z\\ +\dfrac{L}{2}(1-F))]\}, & Z<-L(1-F)/2.\end{cases} \tag{4}$$

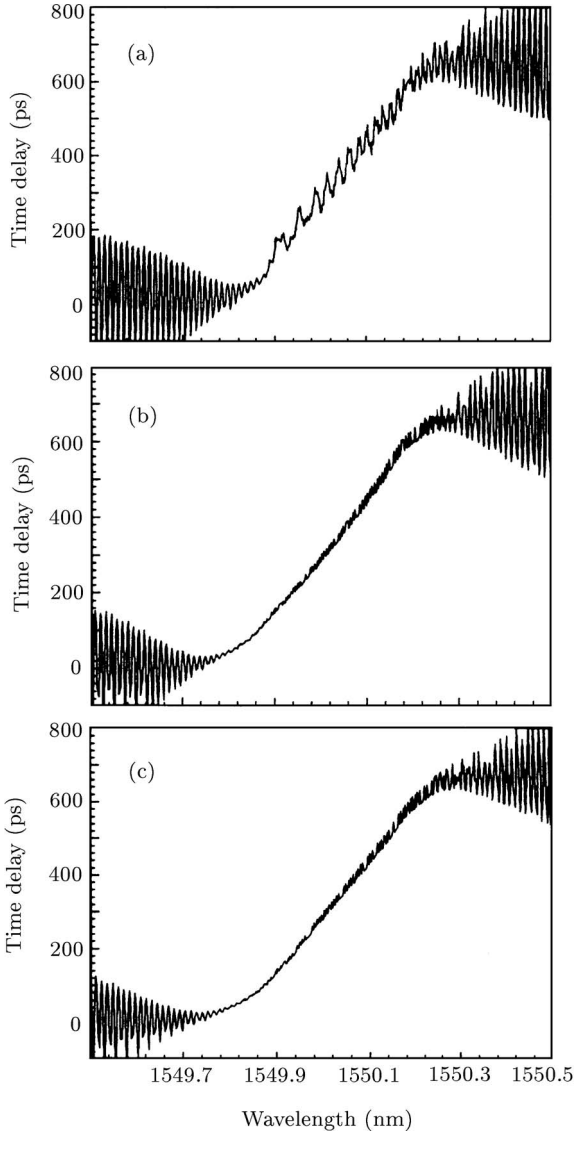


**Fig. 1.** Time-delay characteristics corresponding to different apodization functions: (a) without apodization; (b) with full apodization; (c) with fractional apodization.

As usual, let us refer to Eqs. (1)–(4) as curve groups (1)–(4). Other window functions can be expanded as the curve 4, including the Hamming, Bartlett, Blackman windows. The parameter $F$ in the curves is actually the fraction of the grating length $L$ that is apodized. For example, curve 4 falls to zero at the grating ends and approaches $\overline{\delta}n_{\rm eff}$ toward $Z=\pm(1-F)L/2$. When $F=1$, curve 4 is an exactly Hanning window function and when $F\to 0$, curve 4 is changed to the rectangular window without apodization. The greater values of the parameters of $m$ and $T_1$ in curves 2 and 3 correspond to the profiles of the sharper slope. If the parameter $T_1$ in curve 1 has the greater value, the value of curve 1 at the grating ends is closer to zero. In this letter, the parameter $T_0$ in curve 2 takes the value of $0.8\,L$.

For a definite amount of chirp $\mathrm{d}\lambda_{\rm D}/\mathrm{d}Z$ and the grating length $L$, we define that the optimal profiles should satisfy two conditions: the corresponding time-delay characteristic to the optimal profile has relatively more linearization and broader dispersion bandwidth.

Starting from one of our experiments,[6] the grating parameters are enumerated as follows: $L=100\,\mathrm{mm}$, $\overline{\delta}n_{\rm eff}=0.0002$, $\mathrm{d}\lambda_{\rm D}/\mathrm{d}Z=-0.0022\,\mathrm{nm/mm}$, $\lambda_0=1550.0\,\mathrm{nm}$. If $\overline{\delta}n_{\rm eff}(Z)$ takes the function of curve 1, the optimal profile is found at $F=0.48$ provided that $T_1=100$. Three curves of time-delay characteristics are illustrated in Fig. 1. Figs. 1(a), 1(b) and 1(c) correspond, respectively, to the time-delay characteristics without apodization ($F\to 0$), with full apodization ($F=1$) and with fractional apodization ($F=0.48$). If the same procedure is applied to curves 2, 3 and 4, the parameters corresponding to the optimal profiles are $m=6$, $T_1=0.08$ and $F=0.56$. For the expanded Bartleltt, Blackman and Hamming windows, we have $F=0.39$, 0.59 and 0.56. Among all these optimal profiles, the time-delay characteristics corresponding to the profiles from curves 1, 2 and 3 have more linearization than others. We can get some impression from the comparison between Fig. 1(c) and Fig. 2, which is the time-delay characteristic corresponding to the optimal profile of curve 4. In the process of comparison, close attention should be paid to the fact that the optimal profiles require more linearization and broader dispersion bandwidth in its own profile group. The same principle can be applied to any other comparisons.

Now we consider different lengths of gratings while maintaining the other grating parameters unchanged. For curve 1, the optimal profile of the grating with the smaller grating length requires the greater value of the parameter $F$, assuming $T_1=100$. When $L=45\,\mathrm{mm}$, the optimal profile has the parameter $F=1$ (Fig. 3), which means that when $L<45\,\mathrm{mm}$, there is no optimal profile for the curve 1. There exist similar circumstances for other profiles, i.e. for some definite amount of chirp, there are the corresponding optimal lengths in some range of the grating length. In our instance, for curve 1 ($T_1=100$), the range of the optimal lengths is $45-100\,\mathrm{mm}$ and the parameter $F$ of the optimal profiles changes from 1 to 0.48. In a

practical view, for the grating with the chirp amount 0.0022 nm/mm, the optimal grating length is 45 mm since longer gratings do not substantially improve the quality of the transmitted signal.

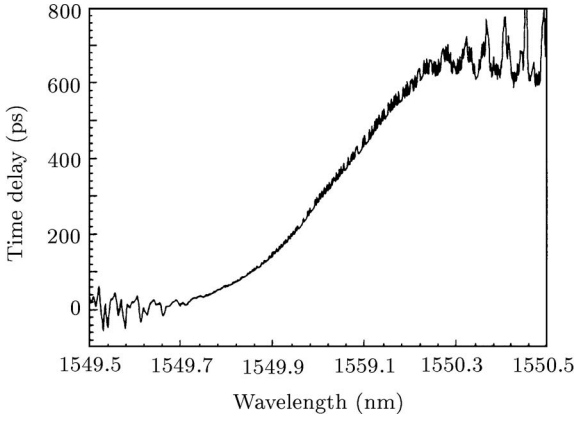


**Fig. 2.** Time-delay characteristic corresponding to the optimal profile of curve 4.

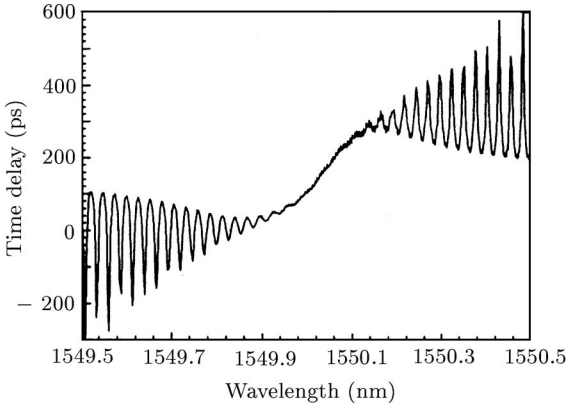


**Fig. 3.** Time-delay characteristic corresponding to the optimal profile when $L = 45$ mm.

There are only four curves shown in Fig. 4 for clarity, which are the curves: $(a)$ $T_1 = 100$, $F = 0.48$ and $(b)$ $T_1 = 100$, $F = 1.0$, where curves $a$ and $b$ come from Eq. (1); $(c)$ $m = 6$ for Eq. 2 and $(d)$ $F = 0.56$ for Eq. 4. It is obvious that from Fig. 4, the sidelobe suppression of the lower curve(s) is better than the sidelobe suppression of the upper curve(s). The sidelobe suppression of the three low curves has surpassed the value smaller than $-30$ dB. Basically, it is suitable for the requirement of the wavelength division multiplexing elements. The greater values of the parameter $T_1$ in curve 1 lead to better sidelobe suppression. $T_1$ in curve 1 plays the role of an adjustable parameter, which is a characteristic different from other profiles. How much the sidelobe suppression is needed depends on the specific instance. Our numerical calculation has shown that the sidelobe suppression level for the optimal profiles can be arranged from the worst to the best as follows: curve 2 ($m = 6$); the expanded Hamming window ($F = 0.56$); curve 1 ($T_1 = 100$, $F = 0.48$); curve 3 ($T_1 = 0.08$); the expanded Bartlett window ($F = 0.39$); curve 4 ($F = 0.56$); and the expanded Blackman window ($F = 0.59$).

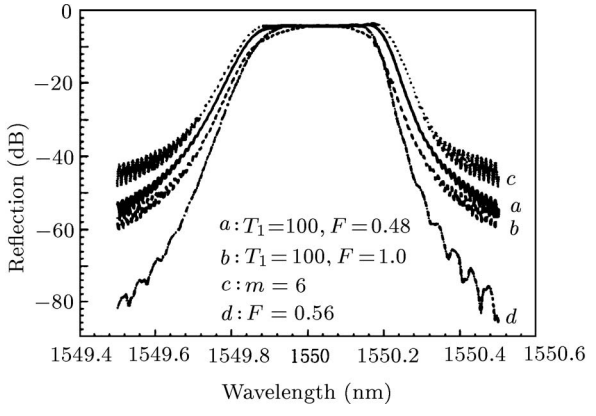


**Fig. 4.** Sidelobe suppression of different profiles.

Qualitatively, the sidelobe suppression is related to how smoothly the profile terminates at the grating ends.[7] The reduction of the oscillation in time-delay characteristics, in this letter, is demonstrated to be related to the parameters: $m$ and $T_1$, respectively, in curves 2 and 3, and $F$ (the fraction of apodization) in the other curves. These factors play an important role in practical designs for dispersion compensators.

In conclusion, starting from our defined profile functions, we find the optimal profiles of different curves. Among them, the time-delay characteristics for the optimal profiles of curves 1, 2 and 3 have more linearization than other curves. The sidelobe suppression level is various for the optimal profiles of different curves, among which curve 1 has its own characteristic due to the adjustable parameter $T_1$. The reduction of the oscillation in time-delay characteristics is demonstrated to be related to the parameters: $m$ and $T_1$, respectively, in curves 2 and 3, and $F$ (the fraction of apodization) in the other curves. Specifically, for curve 1 ($T_1 = 100$) numerical calculations have shown that the optimal grating length is 45 mm, corresponding to the optimal profile, i.e. curve 1 ($T_1 = 100, F = 1$). The method of looking for the optimal grating length is applicable to various circumstances.

# References

[1] Loh W H *et al.* 1995 *Opt. Lett.* **20** 2051
[2] Hill K O *et al.* 1994 *Opt. Lett.* **19** 1314
[3] Mason P L *et al.* 1994 *Electron. Lett.* **30** 1244
[4] Erdogan T 1997 *J. Lightwave Technol.* **13** 1277
[5] Yamada M and Sakuda K 1987 *Appl. Opt.* **6** 3474
[6] Qin Z X *et al.* 1999 *Sci. Chin.* A **42** 883
[7] Cross P S and Kogelnik H 1977 *Opt. Lett.* **1** 43